Design and structure of a novel Neurokinin A receptor antagonist cyclo(-Met^1-Asp^2-Trp^3-Phe^4-Dap^5-Leu^6-)cyclo(2β-5β)

Vincenzo Pavone,*[a] Angelina Lombardi,[a] Flavia Nastri,[a] Michele Saviano,[a] Ornella Maglio,[a] Gabriella D'Auria,[a] Laura Quartara,[b] Carlo Alberto Maggi[b] and Carlo Pedone[a]

[a] *Centro Interdipartimentale di Ricerca su Peptidi Bioattivi, University of Naples 'Federico II', Via Mezzocannone 4, 80134 Napoli, Italy*

[b] *A. Menarini Pharmaceutical Industries, Via Sette Santi 3, 50131 Firenze, Italy*

We report here the rational design, synthesis and structural characterization in the solid state and in solution of the most potent and selective peptide-based Neurokinin A (NKA) antagonist, thus far described. We predicted the bioactive conformation of the known NKA antagonist cyclo(-Met^1-Gln^2-Trp^3-Phe^4-Gly^5-Leu^6-) by comparison with the known structures of other cyclohexapeptides. On this basis we designed a highly constrained peptide molecule corresponding to a bicyclic hexapeptide containing two rings of 14 atoms, namely cyclo(-Met^1-Asp^2-Trp^3-Phe^4-Dap^5-Leu^6-)cyclo(2β-5β). It was synthesized efficiently, using a combined solution and solid phase strategy. We fully characterized this molecule in the solid state by X-ray diffraction and we show that it adopts an almost identical conformation in acetonitrile solution by NMR spectroscopy. This structure fully confirms our hypothetical model. Its structure and conformational rigidity in solution explain the high potency and selectivity and the resistance to proteolytic degradation. Therefore the structural requirements for NKA antagonistic activity are clarified.

Introduction

In order to enhance the biological activity and metabolic stability of bioactive peptides, several attempts have been made to mimic the hypothetical spatial requirements for ligand–receptor interactions, using insight gleaned from NMR, X-ray and computational techniques, coupled with the use of either local constraints (unnatural amino acids or dipeptides, peptidomimetics) or global constraints (cyclization).[1] Both of these approaches have been applied to techykinins (TKs), in order to obtain selective agonists[2-4] or antagonists.[5,6] TKs are a family of peptides widely distributed in the central and peripheral nervous system of amphibians and mammals, where they play a key role in neuronal stimulation.[7] The three mammalians' TKs, Substance P (SP), Neurokinin A (NKA) and Neurokinin B (NKB), act through a preferential interaction with the NK-1, NK-2 and NK-3 receptors, respectively. NKA is involved in bronchoconstriction, smooth muscle contraction and inflammation. Several NKA receptor antagonists have been reported, either peptide[8-10] or non-peptide[11] in nature, which may have a wide range of therapeutic applications.

Recently, McKnight *et al.*[12] described a series of NK-2 receptor antagonists. The most active of the series is L659,877 or cyclo(-Met^1-Gln^2-Trp^3-Phe^4-Gly^5-Leu^6-), formally derived from head-to-tail cyclization of the weak antagonist L659,874 or Ac–Leu-Met-Gln-Trp-Phe-Gly–NH_2. The enhancement of antagonist activity and selectivity derived from cyclization, clearly showed that a favourable conformation for specific interaction with NK-2 receptor was mimicked. Furthermore, two constrained analogues of L659,877, containing the substitution of Gly with Pro and of the dipeptide Gly-Leu with the Gly[(*R*)-γ-lactam]Leu moiety, were described. The antagonist activity of the analogue containing the lactam substitution was approximately ten-fold lower, while the Pro^5 analogue was inactive. Therefore the substitutions inserted perturbed the active conformation of the molecule, and indicated a key role of the Gly residue. In spite of these data, recently a conformational NMR and Molecular Dynamic (MD) study showed for L659,877 and its analogue containing the (*R*)-γ-lactam moiety a wide range of possible conformations in dimethylsulfoxide (DMSO) solution.[13] Looking for a rationalization of the available information, we related these results to the structural data on the conformation of the NKA selective agonist [β-Ala^8]-NKA(4-10) (ref. 14) and [Lys^3,Gly^8(*R*-γ-lactam)Leu^9]NKA(3-10) (GR64349) (ref. 4), in particular for the conformational assessment of the Gly residue. This was based on the *a priori* hypothesis that agonists and a group of antagonists may interact with a comparable three-dimensional structure in the same receptor pocket. Then we postulated the most favourable conformation of L659,877 for interaction with the NK-2 receptor. To confirm our hypothesis, we designed a constrained analogue whose backbone could adopt only a well defined conformation. A second cyclization through β functional groups inserted in positions 2 and 5 was performed, yielding the bicyclic peptide cyclo(-Met^1-Asp^2-Trp^3-Phe^4-Dap^5-Leu^6-)-cyclo(2β-5β) (MEN10627; Dap: 2,3-diaminopropionic acid). The three-dimensional structure of this compound perfectly corresponds to the expected features and, as described elsewhere,[15] MEN10627 is the most potent peptide-based NK-2 receptor antagonist described thus far; it possesses high affinity for the NK-2 receptor, 10–100 fold higher than the parent monocyclic compound at the NK-2 receptor expressed in different species. We describe here the design, synthesis and solution and solid state structure of this new potent and selective NKA antagonist.

Results and discussion

Peptide–receptor interactions depend on several factors, including: (*i*) the three-dimensional structure of the substrate when interacting with the specific receptor; (*ii*) the molecular flexibility; (*iii*) the overall physical-chemical properties. Overall hydrophobicity, as well as high conformational

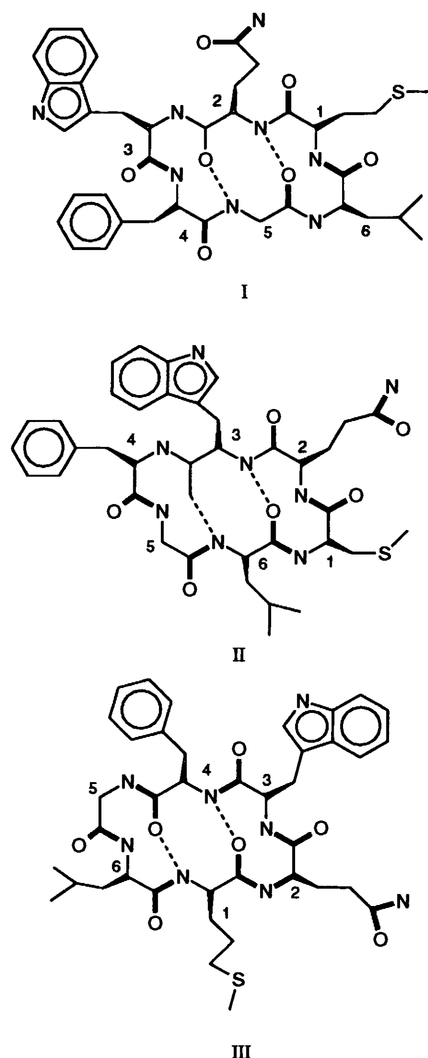

Fig. 1 Schematic representation of hypothetical conformers **I**, **II** and **III** of L659,877

flexibility in solution, are common features among most of the known peptidic NKA antagonists. On the contrary, very little is known of the structural requirements for a best fit into the specific receptor of this class of molecules. We attempted to predict the bioactive conformation for L659,877, one of the most effective peptide based NKA antagonists, by comparison with other known cyclic hexapeptides.

Cyclic hexapeptides have been studied in detail and they are generally characterized in the solid state and in solution by a rectangular or twisted-rectangular shape.[16,17] They often contain two β-turns, positioned on the shortest side of this rectangle and they may be conformationally flexible. This flexibility can be ascribed to a frame shift of hydrogen bonds.[18] We therefore hypothesized that L659,877 may adopt one of the three structures (namely conformer **I**, **II** and **III**) reported schematically in Fig. 1. They differ with respect to the hydrogen bond patterns that are consistent with β-turn structures. The lack of activity in [Pro^5]L659,877, and the overwhelming presence of proline residue at position $i + 1$ of a β-turn in cyclic hexapeptides, allowed us to hypothesize that the bioactive conformation of L659,877 does not correspond to conformer **III**. Furthermore the ring closure associated with lactam formation in [Gly^5(*R*-γ-lactam)Leu^6]L659,877 does not allow the accommodation of Gly(*R*-γ-lactam)Leu segment at position $i + 2$ and $i + 3$ of a β-turn and thus conformer **II** was excluded from further consideration as a bioactive one. In agreement with conformational energy calculations,[4] which indicate for the dipeptide segment Gly(*R*-γ-lactam)Leu a preferred semi-extended conformation, the reduced activity of [Gly^5(*R*-γ-lactam)Leu^6]L659,877 seems to support the hypothesis that conformer **I** may correspond to the bioactive conformation. Successively, a solution NMR study of L659,877 and its derivatives was reported.[13] The molecules display a considerable flexibility in solution adopting a predominant conformation quite different from that proposed here as the bioactive one (conformer **I**). This apparent discrepancy can be ascribed to a small undetectable population of conformer **I** in DMSO solution for L659,877, or to a limited energy conformational search, since most of the detected NOEs, amide proton temperature coefficients and coupling constants are also globally consistent with conformer **I**.

We have also made the arbitrary hypothesis that NKA agonists and antagonists may interact in a similar manner with the NK-2 receptor pocket.

[β-Ala^8]NKA(4-10) is a well known potent and selective agonist and has been well characterized in solution by NMR spectroscopy.[14] It contains two β-turns around the Phe-Val and Leu-Met segments which result in two clusters of hydrophobic amino acids. In this system conformational adjustment of the flexible β-Ala^8 residue from a folded to an extended form would give rise to a molecule almost superimposable to conformer **I**.

To confirm our hypothesis, we designed a constrained analogue whose backbone could adopt only a well defined overall conformation. We also used our previous findings on cyclic peptides containing β-amino acids of 14-membered ring size.[19,20] The model we achieved corresponds to the bicyclic peptide cyclo(-Met^1-Asp^2-Trp^3-Phe^4-Dap^5-Leu^6-)cyclo(2β-5β). Two sets of structures were proposed differing in the orientation of the amide bridge cross linking the side chains of residues 2 and 5 and for the β-turn types around the Trp-Phe and Leu-Met segments. These two different structures were subjected to all-atom energy minimization, and MD simulations and they appeared to be very stable by trajectory analysis and to possess comparable energies (unpublished data).

MEN10627 was synthesized by the Merrifield solid phase method, as summarized in Fig. 2. The classical *N*-α-*t*-Boc (*t*-Boc: *tert*-butoxycarbonyl) strategy was used. The β-amino and β-carboxylic functions of diaminopropionic acid and aspartic acid, engaged in the first cyclization step, were protected as Fmoc (fluoren-9-ylmethoxycarbonyl) and OFm (fluorenyl methyl ester) derivatives, respectively, because they are stable during the acidic treatment for removal of the *t*-Boc group. Met, Trp and Phe residues were incorporated *via* symmetric anhydride; Asp as 1-hydroxybenzotriazole ester and finally Dap was activated by using pyBop [benzotriazol-1-yloxy(tris-pyrrolidinyl)phosphonium hexafluorophosphate]. Before coupling the Met residue, the side chains of Asp and Dap were deprotected with piperidine in dimethylformamide (DMF) and the cyclization was performed on the solid support with pyBop in DMF. After completion of the peptide assembly and removal of the N-terminal *t*-Boc protecting group, the monocyclic peptide was cleaved from the resin by the low–high HF strategy. The second cyclization step was performed in diluted DMF solution using pyBop as the activating agent. The overall yield of the RP-HPLC (reverse phase-high performance liquid chromatography) purified bicyclic peptide was 27%.

The crystal structure of MEN10627 was determined and confirmed that the macrocyclic ring geometry corresponded to conformer **I**. Fig. 3 illustrates a stereo view of the molecule. The geometry for all the residues is in agreement with the literature data. All peptide bonds are *trans*. The backbone atoms of the molecule outline the sides of a rectangle. The Cα atoms of the hydrophobic amino acids are positioned at the corners of the β-turns, resulting in two clusters of hydrophobic groups

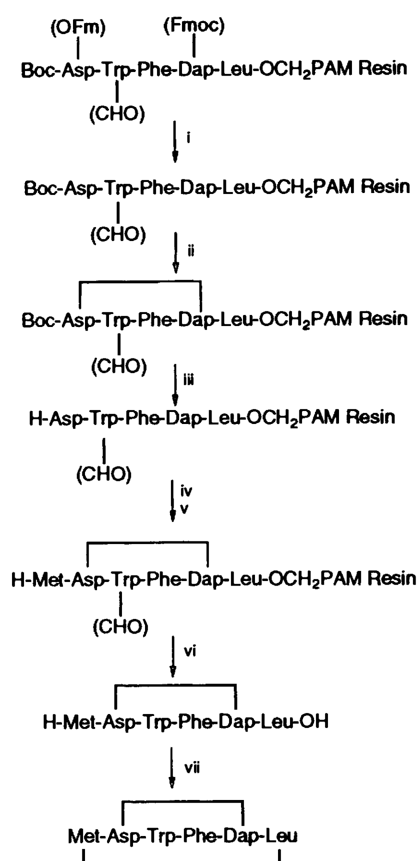

Fig. 2 Synthetic strategy of MEN10627: *Reagents and conditions:* (i) 20% piperidine in DMF (3 + 7 min); (ii) pyBop–DIEA in DMF (12 h); (iii) 50% TFA in DCM (18 min); (iv) *t*-Boc–Met; (v) TFA; (vi) low–high HF: (vii) pyBop–DIEA in DMF (12 h)

corresponding to the side chains of Trp^3, Phe^4 and Leu^6, Met^1, on opposite sides of the cycle and pointing outward from the rectangular core. The torsion angles of the main chain are reported in Table 1. The molecule is characterized by two chain reversals joined by two small stretches of extended conformation. The Trp^3-Phe^4 peptide segment corresponds to a succession of φ, ψ angles close to that of positions 2 and 3 of a slightly distorted type I β-turn. This conformation is stabilized by an intramolecular hydrogen bond involving the CO group of Asp^2 and the NH group of the Dap^5 residue. The molecular conformation of the Leu^6-Met^1 segment corresponds to a succession of φ, ψ angles close to that of positions 2 and 3 of a type II β-turn. This conformation is also stabilized by an intramolecular hydrogen bond involving the NH group of Asp^2 and the CO group of the Dap^5 residue. The Asp^2 and Dap^5 residues are located along the longest sides of the rectangle and they are both in an extended conformation. These residues are hydrogen bonded in a manner similar to that observed in the anti parallel β-sheet.

The Met^1, Phe^4 and Leu^6 side chains adopt typical staggered conformations, while Trp^3 shows a *gauche*(+) χ^1 angle and an unexpected eclipsed χ^2 angle. This can be attributed to packing forces (*vide infra*). The χ^1 angles of Asp^2 and Dap^3 are both *gauche*(+), while the χ^2 angles are both *skew*(−). The particular orientation of the βCO–βNH amide bond is due to hydrogen bond formation. The Asp^2 βCO is a hydrogen bond acceptor of the Phe^4 NH group, while the Dap^5 βNH is hydrogen bonded to the Leu^6 CO group. Therefore the Asp^2-Dap^5 side chain cyclization plays an important role in stabilizing the global conformation, not only for the strong covalent constraint due to amide bond formation, but also for determining the different types (I and II) of β-turns around the Trp^3-Phe^4 and Leu^6-Met^1 segments. Table 2 summarizes both the intra- and inter-molecular hydrogen bonds.

The molecular packing, as seen in stereo view in Fig. 4, is

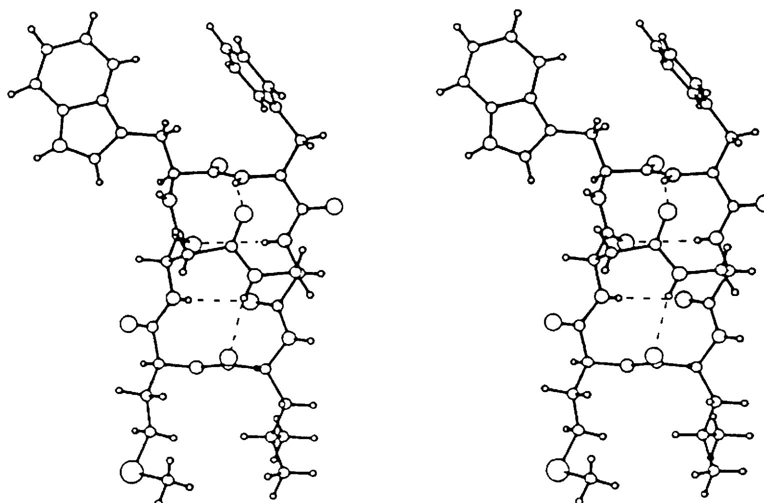

Fig. 3 Stereo view of MEN10627 as derived from X-ray diffraction analysis

Table 1 MEN10627: torsional angles in degrees, derived from the X-ray structure (estimated standard deviations are less than 0.6°)

	Met^1	Asp^2	Trp^3	Phe^4	Dap^5	Leu^6
φ	57.7	−153.5	−59.3	−130.2	−168.2	−64.8
ψ	27.4	172.9	−34.7	40.5	178.5	127.9
ω	177.4	−172.1	−177.9	−168.2	166.4	179.8
χ^1	−54.9	78.7	−65.5	−36.1	70.7	−158.2
$\chi^{2.1}$	−175.0	−79.9^a	−4.7	118.9	−93.9^b	−162.5
$\chi^{2.2}$	−75.3^c	98.6^d	174.8	−59.2	173.7^e	74.5

^{a} C^{α}_2-C^{β}_2-C^{γ}_2-N^{γ}_5. ^{b} C^{α}_5-C^{β}_5-N^{γ}_5-C^{γ}_2. ^{c} χ^3. ^{d} C^{α}_2-C^{β}_2-C^{γ}_2-O^{γ}_2. ^{e} C^{β}_2-C^{γ}_2-N^{γ}_5-C^{β}_5.

Table 2 MEN10627: intra- and inter-molecular hydrogen bonds, derived from the X-ray structure

Intramolecular

Donor	Acceptor	N→O/Å	N-O=C(°)	H→O/Å	D-H→A(°)
N_2	O_5	3.226(4)	110.9(2)	2.46(4)	156.2(6)
N_4	O^{γ}_2	2.978(4)	116.6(2)	2.13(4)	153.1(7)
N_5	O_2	3.321(4)	105.4(2)	2.59(4)	155.3(6)
N^{γ}_5	O_6	3.062(4)	110.0(3)	2.21(4)	167.7(6)

Intermolecular

Donor	Acceptor	D→A/Å	D-A=C(°)	H→A/Å	D-H→A(°)
N_1	$N_{2S}{}^a$	3.087(6)	169.4(3)	2.27(3)	165.0(7)
N_3	$N_{1S}{}^b$	3.213(7)	142.7(3)	2.52(4)	163.7(6)
N^{ε}_3	$O_2{}^c$	3.429(5)	170.2(3)	2.71(4)	135.9(7)
N_6	Ow^a	2.856(5)		2.00(4)	164.4(7)
Ow	$O_4{}^d$	2.810(5)	138.1(5)	1.93(5)	166.1(6)
Ow	$O_6{}^e$	2.784(5)	155.4(3)	1.85(5)	157.4(6)

Symmetry operation: ^{a}: x, y, z; ^{b}: $1/2 - x, 1 - y, 1/2 + z$; ^{c}: $x - 1/2, 3/2 - y, 1 - z$; ^{d}: $x - 1/2, 1/2 - y, 1 - z$; ^{e}: $1/2 + x, 1/2 - y, 1 - z$.

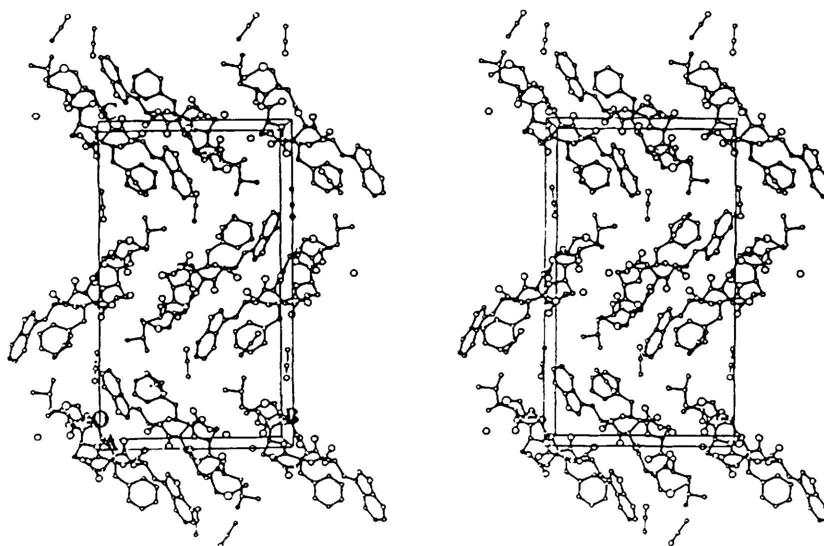

Fig. 4 Stereo view of the molecular packing of MEN10627

characterized by rows of molecules along the *a* direction, held together by a weak hydrogen bond between the indolyl εNH and the αCO group of Asp[2] belonging to symmetry related molecules. Solvent molecules (one of water and two of acetonitrile) further stabilize the crystal packing. In particular the water (Ow) is strongly hydrogen bonded to N_6H, O_4 and O_6 in an approximately pyramidal arrangement. The nitrogen atoms of both acetonitrile molecules are hydrogen bond acceptors from the N_1H and N_3H groups. These solvent molecules also are in close van der Waals contact with several surrounding atoms.

It is well known that linear or cyclic peptides may adopt in the solid state a conformation different from that in solution and therefore we have also analysed the conformational behaviour of MEN10627 in acetonitrile solution.

Resonance assignments, coupling constants and the temperature gradient of amidic NH protons are reported together with spin–lattice relaxation times in Table 3.

An examination of the connectivities derived from NOE data suggests regularity in elements of the MEN10627 secondary structure. The T_1 relaxation times for the α-carbons are uniform, indicating that the peptide backbone is rigid and is undergoing isotropic molecular reorientation on the Larmor timescale. The observations of an NOE between NH–Phe[4]-NH–Dap[5] and a weaker NOE between NH–Trp[3]-NH–Phe[4], together with the small $^3J_{NH\text{-}\alpha}$ coupling constant of Trp[3] and the large $^3J_{NH\text{-}\alpha}$ of Phe[4] are all consistent with the theoretical values for a type I β-turn. The very small temperature coefficient of Dap[5] amidic αNH is consistent with a hydrogen bond, presumably between NH–Dap[5] and CO–Asp[2] for a characteristic β-turn structure enclosing the Trp[3]-Phe[4] segment. A quite strong NOE between NH–Met[1]-NH–Asp[2] supports the existence of a II/II′ β-turn with Leu[6]-Met[1] at the corner positions. It is stabilized by a hydrogen bond from NH–Asp[2] to CO–Dap[5], as confirmed by a small temperature coefficient for amidic NH–Asp[2]. The coupling constants $^3J_{NH\text{-}\alpha}$ of Leu[6] and Met[1] are in agreement with a type II β-turn as the first constant is small (possible φ solution of the Karplus relationship is $-60°$) and the second is 7.1 Hz for which a possible solution is a positive φ value ($+60$). Furthermore, the low temperature coefficient of Met[1] amide proton is consistent with a type II β-turn since, in this particular secondary structure, this proton is partially solvent shielded and weakly interacting with the CO group corresponding to the first position of the turned structure (Dap[5]) ($N_1 \rightarrow O_5$ is of about 3.2 Å). Relatively small temperature coefficients are also exhibited by Phe[4] and βNH–

Table 3 Chemical shifts,[a] coupling constants, amide proton temperature coefficients and spin–lattice relaxation time[b] for MEN10627

Residue		δ_H	δ_C	J/Hz	$\Delta\delta_{NH}/\Delta T$/ppb K^{-1}	$^{13}C\ T_1$/s
Met[1]	NH	7.68		NH-α = 7.1	−1.8	
	αCH	4.14	52.1	αβ = 4.3		0.5
	β*proS*	2.20	29.2	αβ′ = 8.5		0.6
	β*proR*	1.90				
	γγ′	2.43	30.3			1.0
	SCH_3	2.04				
Asp[2]	NH	7.12		NH-α = 6.4	0	
	αCH	4.58	49.9	αβ = 4.8		0.45
	β*proS*	2.75	39.1	αβ′ = 3.6		0.44
	β*proR*	2.60		ββ′ = 13.3		
Trp[3]	NH	7.18		NH-α = 4.0	−4.0	
	αCH	4.22	56.8	αβ = 9.0		0.49
	ββ′	2.98, 2.92	26.6	αβ′ = 5.8		0.46
	2H-7H	7.02–7.49		ββ′ = −15.2		
	εNH	9.16			−3.0	
Phe[4]	NH	7.61		NH-α = 8.4	−1.3	
	αCH	4.45	53.9	αβ′ = 9.3		0.5
	β*proS*	3.33	36.4	αβ = 5.3		0.48
	β*proR*	2.69		ββ′ = −13.9		
	2H-6H	7.16–7.25				
Dap[5]	NH	7.06		NH-α = 7.2	0	
	αCH	4.49	53.5	αβ = 3		0.45
	β	3.93	40.7	αβ′ = 1		0.40
	β′	3.56		ββ′ = −12.7		
	βNH	6.84		NH-β = 6.0	−1.2	
Leu[6]	NH	7.10		NH-α = 5.0	−4.2	
	αCH	4.09	54.7	αβ = 7.0		0.45
	ββ′	1.58, 1.49	39.3	αβ′ = 8.4		0.45
	γCH	1.67	24.5	ββ′ = −13.3		0.8
	δCH_3	0.96	21.8			
	$\delta' CH_3$	0.92	21.2			

[a] ^1H Chemical shifts referred to Me_4Si; ^{13}C chemical shifts referred to CD_3CN at 0.3 ppm. [b] CT_1 values reported as NT values where N is the number of attached hydrogens and T is the spin–lattice relaxation time.

Table 4 Relevant interprotonic distances (Å) from experimental NOEs for MEN10627; *pro-R* and *pro-S* chiralities of βCH protons are specified by *R* and *S*

Residue	1	2	3	4	5	6
N_iN_{i+1}	2.7		3.2	2.8		
$N_i\alpha_i$	n.e.[a]	3.4	3.3	2.6	n.e.	2.8
α_iN_{i+1}	3.4	2.6	2.6	2.7	2.7	n.e.
$N_i\beta_i$	3.3*R*	3.6*S*	2.4*R* 3.0*S*	3.0*R*		
β_iN_{i+1}		2.2*R* 2.9*S*	3.2*S*		2.3*R*	
$\alpha_i\beta_i$	2.6*S* 2.9*R*	2.4*S* 2.3*R*	2.9*S* 2.6*R*	2.5*S* 3.0*R*	2.4*S* 2.4*R*	

[a] n.e. denotes unevaluated distances for spectral overlapping.

Dap[5] amide protons. A possible explanation for these low values is the formation of hydrogen bonds with the β-CO of Asp[2] and CO of Leu[6].

Some relevant inter-proton distances estimated from NOEs are reported in Table 4. Except for the NH–Phe[4]-αCH–Trp[3] distance, that is found to be shorter than expected, all distances differ by less than 0.4 Å from values derived from the X-ray study. Within the experimental error (10% on NOE derived distances) high structural homology in the solid state and in solution is suggested; major differences are due to the different Trp[3] and Leu[6] side chain rotamer populations in solution. The eclipsed χ^1 conformation observed in the solid state for Trp[3] is due to inter-molecular interactions, while in solution the more stable *trans* conformation is observed. Finally, all NMR experimental observations, coupling constants, NOEs and temperature coefficients, are in agreement with a three-dimensional structure in CD_3CN solution almost identical to that observed in the solid state. Therefore a restrained molecular dynamic calculation, generally applied to refine the NMR models, seems unnecessary in this case.

In conclusion, by predicting the bioactive conformation of the NKA receptor antagonist L659,877 and its analogues, we designed rationally a highly constrained peptide molecule. It corresponds to a bicyclic hexapeptide containing two rings of 14-atoms. It was efficiently synthesized, using a combined solution and solid phase strategy. This molecule adopts an almost identical conformation in the solid state and in solution. It fulfills the following structural requirements: (*i*) it is sufficiently hydrophobic to ensure absorption by the target tissue; (*ii*) it is conformationally inflexible (at least as regards the backbone chain) to provide high affinity and selectivity for the NK-2 receptor; (*iii*) it possesses the right orientation of the hydrophobic side chains to provide an optimum fit into the receptor pocket. We have thus demonstrated the structural requirements for NKA receptor antagonistic activity. Furthermore the conformational rigidity, detected by NMR spectroscopy, may explain the high potency of MEN10627 in *in vivo* experiments:[15] the unexpected long lasting activity can be attributed to a high degree of resistance to peptidases, since it is reasonable to believe that the rigid structure of MEN10627 neither fits, nor can be adapted to, the active site of peptidases. Finally the postulated structural similarity between NKA peptide agonists and antagonists will be of great help in understanding their different biological behaviours.

Experimental

Synthesis

The synthesis of MEN10627 was achieved by the solid phase method (0.5 mmol scale), on an Applied BioSystems Model

430A automatic peptide synthesizer. The classical protocols for *N*-α-*t*-Boc strategy were used. The peptide chain was assembled, on a *t*-Boc–Leu–OCH_2–Pam resin (Pam: phenylacetamidomethyl), by consecutive addition of *t*-Boc–Dap-(β-Fmoc)–OH,[21] *t*-Boc–Phe–OH, *t*-Boc–Trp–(CHO)–OH, *t*-Boc–Asp-(β-OFm)–OH and *t*-Boc–Met–OH. All amino acids, except *t*-Boc–Dap-(β-Fmoc)–OH and *t*-Boc–Asp-(β-OFm)–OH, were incorporated *via* symmetric anhydrides by using a dicyclohexylcarbodiimide–dichloromethane (DCC–DCM) solution. *t*-Boc–Asp-(β-OFm)–OH was activated to the 1-hydroxybenzotriazole ester. *t*-Boc–Dap-(β-Fmoc)–OH was coupled according to the pyBop procedure.[22,23] *t*-Boc protecting groups were removed by the usual trifluoroacetic acid (TFA) treatment.

Before coupling the *t*-Boc–Met–OH residue, the side chains of Asp and Dap were deblocked with piperdine in DMF (20% v/v; 3 + 7 min) and the linear precursor was cyclized on the solid support by treatment with pyBop (3 equiv.) and DIEA (diisopropylethylamine; 6 equiv.) in DMF overnight.[24]

After removal of the N-terminal *t*-Boc, coupling of *t*-Boc–Met–OH was performed and then followed by treatment with TFA. Trp side chain deprotection with concomitant cleavage of the monocyclic peptide from the resin was achieved with the low/high HF procedure.[25] The crude product was extracted in aq. acetic acid (50% v/v) and the resultant solution was lyophilized. 310 mg of crude material were obtained (yield 80%) and it was successively purified by preparative RP-HPLC on a Water Delta Prep 3000 apparatus, Vydac C_{18} column (50 × 250 mm; 10 μm), H_2O–CH_3CN (0.1% TFA) linear gradient. 145 mg (0.186 mmol; yield 37%) of monocyclic peptide were obtained. Analytical RP-HPLC on a Varian 3000 LC Star System, equipped with a Vydac C_{18} column (4.6 × 150 mm; 5 μm) confirmed the purity of the product. Fast atom bombardment mass spectroscopy (FABMS) gave a molecular ion peak $[M - H]^+$ of 779 amu as expected.

The second cyclization step was performed in dilute DMF (1 mmol dm^{-3}), using pyBop as activating reagent. 0.183 mmol of monocyclic peptide were allowed to react in 183 cm^3 of dry DMF, with 1 equiv. of pyBop and 3 equiv. of DIEA, at room temperature, overnight. The solvent was evaporated *in vacuo* and the product was lyophilized. After purification by preparative RP-HPLC, in the same conditions described above, 107 mg (0.141 mmol, cyclization yield 77%, overall yield 27%) of bicyclic peptide were obtained. FABMS confirmed the molecular weight: $[M - H]^+$ of 761 amu.

Data collection and processing

The X-ray study was performed using graphite monochromated Cu-Kα radiation ($\lambda K\alpha = 1.5418$ Å) on an Enraf-Nonius CAD4 diffractometer equipped with a MicroVax 3100 Server Digital computer. Single crystals were grown by slow evaporation of a CH_3CN solution at room temperature. Because the crystals deteriorated rapidly upon drying, they were sealed in thin-walled glass capillaries in contact with their mother liquor. Crystal data: molecular formula $C_{38}H_{48}N_8O_7S \cdot H_2O \cdot 2CH_3CN$; $M = 861.04$ (amu); crystal system: orthorhombic; space group: $P2_12_12_1$; $Z = 4$ (formula weight/unit cell); $a = 10.058(2)$, $b = 16.117(2)$, $c = 27.911(5)$ Å; $V = 4525(2)$ Å^3; $D_{calc.} = 1.264$ g cm^{-3}. Data collection was performed with a standard procedure.[26] 4796 Total independent reflections were collected in the θ range 1–70°; 3757 of which having a net intensity greater than $3.0\sigma(I)$ were considered observed and used for further calculation.

Structure solution

The structure was solved with SIR92,[27] using the random phase procedure. The best solution revealed all non-hydrogen atoms of MEN10627. Subsequent difference Fourier analysis revealed the presence of one water and two acetonitrile co-crystallized molecules, and all hydrogen atoms. The structure was refined with anisotropic thermal parameters for the C, O, N, S atoms, while the hydrogen atom coordinates were refined with a fixed isotropic temperature factor equal to the equivalent *B* factor of the heavy atom to which they are linked, using the SDP package.[28] A full-matrix least-squares procedure was used, converging to a final *R* factor of 0.044 and *Rw* of 0.042 with anisotropic displacement factors for the non-hydrogen atoms. The atomic coordinates of MEN10627 together with the equivalent *B* factors, bond lengths, bond angles and torsion angles have been deposited.† Atomic scattering factors employed were calculated from ref. 29.

NMR analysis

^1H NMR 1D and 2D experiments were recorded on a Varian Unity 400 spectrometer, operating at 400 MHz and equipped with a Sparc Station SUN 330. NMR spectra were recorded at 298 K from 8 mmol dm^{-3} CD_3CN solution. Phase sensitive 2D experiments (DQF-COSY,[30] HOHAHA,[31] NOESY[32]) were performed according to the States–Haberkorn method. A mixing time of 70 ms was used for HOHAHA experiments. NOESY experiments were acquired at 100, 150 and 300 ms. Proton spin system assignments were achieved by using a combination of scalar and dipolar correlation 2D experiments.[33] ^{13}C NMR data were obtained from a heteronuclear multiple quantum correlation (HMQC) experiment.[34] ^{13}C T_1 values were determined using an inversion recovery sequence. The temperature coefficients of Met^1 and Phe^4 amidic NH protons were obtained from 1D spectra. For the other residues the $\Delta\delta/\Delta T$ values were extracted from a series of 2D spectra and checked at higher resolution with 1D-TOCSY spectra recorded at a different temperature. The temperature coefficients obtained at 8 mmol dm^{-3} were confirmed at lower concentrations (2 and 1 mmol dm^{-3}). Except for Leu^6, the χ_1 angles were defined for all residues according to their patterns of $^3J_{\alpha\beta}$ coupling constants and NH-β,αβ NOESY cross peak intensities.[35] The NOESY experiments yielded about 40 NOE contacts in positive regime. Cross relaxation rates for each spin pair were obtained by the initial build-up rate approximation.[36] The Phe^4 ββ′ CH_2 distance of 1.78 Å was used as a reference.

While this manuscript was under consideration for publication, three papers appeared in the literature[37–39] on the conformational analysis in solution of L659, 877. They confirm our hypothesis on the L659, 877 bioactive conformation.

† For details of the CCDC deposition scheme, see 'Instructions for Authors (1995)', *J. Chem. Soc., Perkin Trans. 2*, 1995, issue 1.

References

1 V. J. Hruby, F. Al-Obeidi and W. Kazmieski, *Biochem. J.*, 1990, **268**, 249.
2 C. Gilon, A. Halle, M. Chorev, Z. Selinger and G. Byk, *Biopolymers*, 1991, **31**, 745.
3 G. Holzemann, A. Jonczyk, V. Eiermann, K. G. R. Pachler, G. Barnickel and D. Regoli, *Biopolymers*, 1991, **31**, 691.
4 M. J. Deal, R. M. Hagan, S. J. Ireland, C. C. Jordan, A. B. McElroy, B. Porter, B. C. Ross, M. Stephens-Smith and P. Ward, *J. Med. Chem.*, 1992, **35**, 4195.
5 P. Ward, G. B. Ewan, C. C. Jordan, S. J. Ireland, R. M. Hagan and J. R. Brown, *J. Med. Chem.*, 1990, **33**, 1848.
6 B. J. Williams, N. R. Curtis, A. T. McKnight, J. J. Maguire, S. C. Young, D. F. Veber and R. Baker, *J. Med. Chem.*, 1993, **36**, 2.
7 C. A. Maggi, R. Patacchini, P. Rovero and A. Giachetti, *J. Auton. Pharmacol.*, 1993, **13**, 23.
8 P. Rovero, V. Pestellini, C. A. Maggi, R. Patacchini, D. Regoli and A. Giachetti, *Eur. J. Pharmacol.*, 1990, **175**, 113.
9 A. B. McElroy, S. P. Clegg, M. J. Deal, G. B. Ewan, R. M. Hagan, S. J. Ireland, C. C. Jordan, B. Porter, B. C. Ross, P. Ward and A. R. Whittington, *J. Med. Chem.*, 1992, **35**, 2582.

10 C. A. Maggi, L. Quartara, R. Patacchini, L. Giuliani, G. Barbanti, D. Turini and A. Giachetti, *Regulatory Peptides*, 1993, **47**, 151.
11 X. Edmonds-Alt, P. Vilain, P. Goulaouic, V. Proietto, D. Van Boeck, C. Advenier, E. Naline, G. Neliat, G. Le Fur and J. C. Breliere, *Life Science*, 1992, **50**, PL-101.
12 A. T. McKnight, J. J. Maguire, N. J. Elliott, A. E. Fletcher, R. Foster, R. Tridgett, B. J. Williams, J. Longmore and L. L. Icersen, *Br. J. Pharmacol.*, 1991, **104**, 355.
13 U. Wollborn, R. M. Brunne, J. Harting, G. Holzemann and D. Leibfritz, *Int. J. Peptide Protein Res.*, 1993, **41**, 376.
14 G. Saviano, P. A. Temussi, A. Motta, C. A. Maggi and P. Rovero, *Biochemistry*, 1991, **30**, 10175.
15 C. A. Maggi, M. Astolfi, S. Giuliani, C. Goso, S. Manzini, S. Meini, R. Patacchini, V. Pavone, C. Pedone, L. Quartara, A. R. Renzetti and A. Giachetti, *J. Pharmacol. Exp. Th.*, 1994, **271**, 1489.
16 V. Pavone, A. Lombardi, M. Saviano, B. Di Blasio, F. Nastri, R. Fattorusso, O. Maglio and C. Isernia, *Biopolymers*, 1994, **34**, 1505.
17 V. Pavone, A. Lombardi, M. Saviano, F. Nastri, R. Fattorusso, O. Maglio, C. Isernia, L. Paolillo and C. Pedone, *Biopolymers*, 1994, **34**, 1517.
18 M. Gurrath, G. Müller, H. Kessler, M. Aumailley and R. Timpl, *Eur. J. Biochem.*, 1992, **210**, 911.
19 V. Pavone, A. Lombardi, X. Yang, C. Pedone and B. Di Blasio, *Biopolymers*, 1990, **30**, 189.
20 B. Di Blasio, A. Lombardi, G. D'Auria, M. Saviano, C. Isernia, O. Maglio, L. Paolillo, C. Pedone and V. Pavone, *Biopolymers*, 1993, **33**, 621.
21 F. Al-Obeidi, A. M. de L. Castrucci, M. E. Hadley and V. J. Hruby, *J. Med. Chem.*, 1989, **32**, 2555.
22 A. Fournier, C.-T. Wang and A. M. Felix, *Int. J. Peptide Protein Res.*, 1988, **31**, 86.
23 J. Coste, D. Le-Nguyen and B. Castro, *Tetrahedron Lett.*, 1990, **31**, 205.
24 A. M. Felix, C.-T. Wang, E. P. Heimer and A. Fournier, *Int. J. Peptide Protein Res.*, 1988, **31**, 231.
25 J. P. Tam, W. F. Heath and R. B. Merrifield, *J. Am. Chem. Soc.*, 1983, **105**, 6442.
26 V. Pavone, A. Lombardi, G. D'Auria, M. Saviano, F. Nastri, L. Paolillo, B. Di Blasio and C. Pedone, *Biopolymers*, 1992, **32**, 173.
27 A. Altomare, G. Cascarano, C. Giacovazzo, A. Guagliardi, G. Polidori, M. C. Burla and M. Camalli, *J. Appl. Crystallogr.*, 1994, **27**, 435.
28 B. A. Frenz and Associates Inc., Structure Determination Package, A System of Computer Programs, College Station, TX, and Enraf-Nonius, Delt, Holland, 1986.
29 D. T. Cromer and J. T. Waber, *International Tables for X-Ray Crystallography*, Kynoch Press, Birmingham, 1984, vol. 4, table 2.2B, p. 99.
30 U. Piantini, O. W. Sørensen and R. R. Ernst, *J. Am. Chem. Soc.*, 1982, **104**, 6800.
31 A. Bax and D. G. Davis, *J. Magn. Reson.*, 1985, **65**, 355.
32 J. Jeener, B. H. Meier, P. Bachman and R. R. Ernst, *J. Chem. Phys.*, 1979, **71**, 4546.
33 K. Wüthrich, *NMR of Proteins and Nucleic Acids*, Wiley, New York, 1986.
34 M. F. Summer, L. G. Marzilli and A. Bax, *J. Am. Chem. Soc.*, 1986, **108**, 4285.
35 G. M. Clore and A. M. Gronenborn, *Crit. Rev. Biochem. Mol. Biol.*, 1989, **24**, 479.
36 D. Neuhaus and M. Williamson, *The Nuclear Overhauser Effect in Structural and Conformational Analysis*, VCH, New York, 1989.
37 T. J. Siahaan and K. Lutz, *J. Pharmacol. Biomed. Anal.*, 1994, **12**, 65.
38 H. Zhang, T. P. Quinn and T. C. Wong, *Biopolymers*, 1994, **34**, 1165.
39 P. Amodeo, P. Rovero, G. Saviano and P. A. Temussi, *Int. J. Peptide Protein Res.*, 1994, **44**, 556.

Paper 4/06830K
Received 8*th November* 1994
Accepted 20*th December* 1994